INVOTEK

Jurnal Inovasi Vokasional dan Teknologi

http://invotek.ppj.unp.ac.id/index.php/invotek

Vol. 25, No. 1, Feb 2025

ISSN: 1411 – 3411 (p)
ISSN: 2549 – 9815 (e)

# Performance Analysis of FRP Reinforced Concrete After Corrosion Damage

**Achmad Zultan Mansur**[1] *

[1] Department of Civil Engineering, Borneo Tarakan University
Jl. Amal Lama No. 1, Tarakan, Indonesia-77123

*Corresponding author: achmadzultan@gmail.com

Doi: https://doi.org/10.24036/invotek.v25i1.1262



## Abstract

Corrosion in bridge girder beams frequently leads to significant structural damage, such as concrete spalling and reduced reinforcement, which directly impacts the bending capacity. This study experimentally assessed the efficacy of a combined repair strategy of grouting and Glass Fiber Reinforced Polymer (GFRP) reinforcement on simulated damaged reinforced concrete beams. Twelve beams were tested with various repair configurations, including a standalone grouting repair and a combination of grouting with GFRP in strip and U-wrap configurations. The primary objective was to comprehensively evaluate the enhanced flexural capacity and failure modes of these repaired beams. The results indicated that GFRP reinforcement, particularly the U-wrap configuration, significantly improved the beams' flexural capacity. Beams with the GFRP U-wrap configuration achieved an average maximum load of 32.50 kN, surpassing the control beam's 29.74 kN by 9.27%. Conversely, a standalone grouting repair drastically decreased the load capacity to 14.49 kN, highlighting its inefficiency in strength restoration. Debonding failure at the grout-concrete interface was identified as the primary cause of this reduction. The U-wrap configuration outperformed the strip configuration, likely due to its enhanced shear resistance and confinement. The GFRP strain analysis showed linear behavior at low loads but significant deviations at higher loads, which indicates debonding. All beams exhibited a dominant flexural cracking failure mode, with the addition of GFRP reducing the number of cracks. In conclusion, the combined grouting and GFRP reinforcement, especially the U-wrap configuration, proved to be an effective strategy for repairing damaged RC beams. However, achieving strong adhesion between the repair materials and the concrete is crucial to prevent debonding and optimize structural performance. Further research on enhancing adhesion and optimizing GFRP configurations is recommended.

**Keywords:** RC Beams, Grouting, GFRP, Crack Patterns.

## 1. Introduction

Bridge design and construction is a complex process that involves various technical aspects and requires careful consideration. Structural engineers must consider soil conditions, the geographical environment, and the traffic loads the bridge will bear. A primary component in bridge structures is the girder beam, which serves as the main load-bearing element. Girder beams are typically made of high-strength steel or reinforced concrete to withstand dynamic and static loads throughout their service life [1]. However, despite their inherent durability, girder beams are highly susceptible to corrosion, especially when exposed to aggressive environments like coastal areas or those with high pollution levels. Corrosion can cause severe structural damage, such as spalling of the concrete surface covering the girder beam. Spalling occurs when the volume expansion of the formed rust is greater than the original metal, generating internal stresses that cause the protective concrete layer to peel or rupture [2].

Corrosion of girder beams is often triggered by chloride ion ($Cl^-$) attack, originating from dissolved salts in seawater or salt-contaminated water. These chloride ions can penetrate the protective concrete layer through cracks or pores, damaging the passive layer that protects the internal steel reinforcement [2]. This process, known as pitting corrosion, is a highly destructive form of localized corrosion that can lead to deep penetration of the metal. Additionally, water can enter concrete through two primary mechanisms: direct infiltration through impermeable concrete surfaces and transport

Received date 01/06/2025, Revised date 23/07/2025, Accepted date 05/08/2025

through concrete pores. The presence of cracks and pores makes concrete highly susceptible to the penetration of chloride ions and oxygen, which accelerates the reinforcement corrosion process [3]. The carbonation process also accelerates corrosion by lowering the concrete's pH, which in turn damages the reinforcement's passivation layer and enables corrosion reactions to occur. The corrosion reaction of rebar involves an oxidation-reduction (redox) process where iron (Fe) loses electrons to form positive iron ions ($Fe^{2+}$). These ions then react with hydroxide ions ($OH^-$), which are formed from the reaction of oxygen and water, to produce a yellowish-brown, porous iron oxide or rust compound ($Fe_2O_3.H_2O$). This compound has significantly lower mechanical strength than the original iron, leading to a reduction in structural strength and deformation of the reinforcement [2], [4]. This phenomenon—the reduction of the reinforcement's cross-section due to corrosion and the accompanying concrete spalling—directly diminishes the effective area of the tensile reinforcement and the integrity of the concrete cover, thereby significantly reducing the beams' bending capacity and rigidity. The formation of these corrosion products also causes internal stresses in the concrete due to swelling, which triggers further spalling and cracking of the concrete cover. These cracks accelerate the penetration of oxygen, water, and chloride ions into the concrete, exacerbating the corrosion damage [5]. This condition is hazardous as it can reduce the bridge's service life and increase the risk of structural failure.

Effective repair methods and the use of corrosion-resistant materials are crucial for addressing the pervasive issue of corrosion in bridge girder beams and other reinforced concrete structures [6], [7]. Traditional repair techniques include cleaning corroded metal surfaces, applying anti-corrosion coatings, or replacing damaged sections. However, a focus on cost-effectiveness, ease of application, and long-term durability necessitates the exploration of more innovative solutions. Non-shrink cement grouting is recognized for its ability to fill voids and consolidate damaged areas. Concurrently, external reinforcement with composite materials, such as Fiber Reinforced Polymer (FRP) and particularly Glass Fiber Reinforced Polymer (GFRP), has demonstrated significant improvements in both tensile and flexural capacities. The synergistic potential of combining these two methods has also been explored in several studies [6], [8].

Despite these advancements, a comprehensive understanding of the flexural performance of beams that have experienced spalling and reinforcement reduction—simulating damage commonly caused by corrosion—and are subsequently repaired by grouting and reinforced with various GFRP configurations, remains an area requiring further investigation [9]. This study explicitly addresses how such simulated damage, which includes a 38.5% reduction in the tensile reinforcement area by replacing D13 reinforcement with D8 and a simulation of concrete spalling, can be effectively mitigated using a combination of these repair and strengthening methods. The intricate balance between increased strength and potential alterations in ductility and failure modes also warrants a deeper examination. Therefore, this research aims to experimentally evaluate the effectiveness of combining grouting repair and GFRP reinforcement (with various configurations) on the flexural capacity and failure modes of simulated corrosion-damaged reinforced concrete beams. The findings from this study are expected to provide quantitative data and crucial insights for engineers in selecting and designing optimal, safe, and sustainable repair and retrofitting systems for bridge infrastructure.

## 2. Research Method

### *2.1 Specimen and Material Preparation*

This study begins with the preparation of reinforced concrete (RC) beam specimens, which are systematically designed to examine the effect of repair and strengthening methods on structural performance. A total of 12 beams, comprising four variations, were produced. The beams have cross-sectional dimensions of 150×250 mm and an effective length of 3000 mm. They were cast using ready-mix concrete with an average compressive strength of 21 MPa at 28 days, in accordance with ASTM C39 standards. The specimens were divided into a control group and a repaired and strengthened variation group, following the procedure applied in the studies by Attia et al. [10] and Afanda et al. [11], which emphasized the importance of controlling material and geometric variables for the validity of the results. Figure 1 shows a sketch of the steel reinforcement used, with diameters of 13 mm and 8 mm and characterized mechanical properties. This is in line with the study by Lu et al. [12], which demonstrated the effect of steel's yield strength and elastic modulus on the flexural behavior of beams. The careful preparation of these materials and specimens is a crucial foundation for ensuring the consistency and

P-ISSN: 1411-3414
E-ISSN: 2549-9815

accuracy of the test results, as highlighted by Taheri-Shakib et al. [13] in their study on the effect of material variation on reinforced concrete beams.

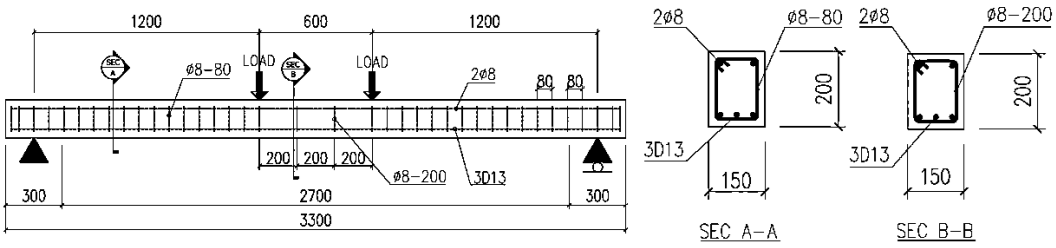


Figure 1. Control beam (RC) Details and Dimensions

### *2.2 Repair and Reinforcement Methods*

The repair and strengthening of beams subjected to damage from corrosion and working loads were performed using approaches proven effective in the existing literature. The RC beam specimens in this study were designed to simulate beams that have undergone spalling and reinforcement reduction due to damage. The primary difference from the control beam is the tensile reinforcement area, which was reduced by 38.5% in the variation beams by replacing the D13 reinforcement with D8. This reduction was realized through the replacement of D13 to D8 reinforcement. Figure 2a illustrates the repair of a reinforced concrete beam using Sikagrou-215 (RBGR), a non-shrink grouting cement capable of filling voids and gaps. This method follows the approach outlined by Wakjira et al. [6] and Koushfar et al. [14], who demonstrated improved structural integrity after grouting application. External reinforcement using GFRP sheets was applied to the beam surface in various configurations. These include a bottom-layer installation (RBGS), as shown in Figure 2b, and a combination of the bottom layer with a U-wrap at the support area (RBGT), as shown in Figure 2c. This protocol follows the methods developed by Siwowski et al. [1] and Capozucca et al. [7]. This combined method of grouting and FRP reinforcement has been experimentally proven to improve flexural capacity and damage resistance, as demonstrated by Jagadheeswari et al. [15]. This approach is expected to provide an effective and economical repair solution for degraded reinforced concrete structures.

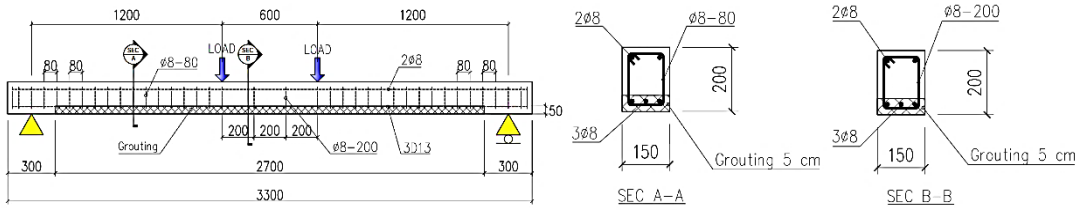


(a) RBGR Variation Type

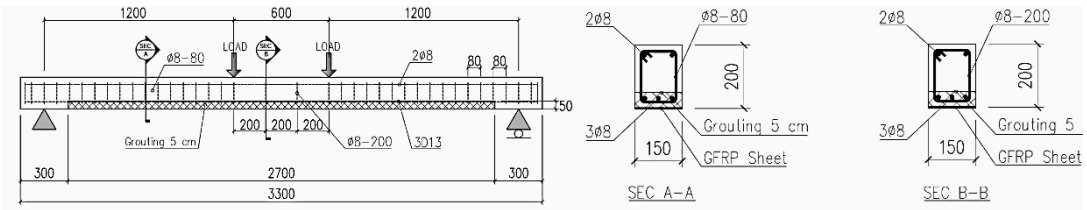


(b) RBGS Variation Type

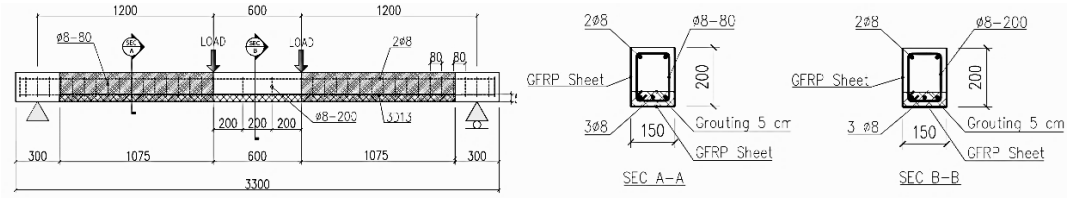


(c) RBGT Variation Type

Figure 2. Details and Dimensions of Variation Beams

P-ISSN: 1411-3414
E-ISSN: 2549-9815

In this study, strain gauges and deflection gauges were used to measure the strain on the reinforcement and concrete surface, as well as the deflection, during bending tests. Data were continuously collected using a digital data acquisition system. For the tensile tests on GFRP, a 1000 kN Universal Testing Machine (UTM) with a loading rate of 0.5 mm/sec was used to obtain a quasi-static response. The GFRP specimens were fabricated using the hand layup method to simulate field conditions.

### *2.3 Experimental Testing Procedure*

The experimental tests, as shown in Figure 3, were conducted using standardized procedures to obtain comprehensive and accurate data on beam performance. The beams were placed on supports with a spacing of 3000 mm and were subjected to a gradual, centralized load until failure. This flexural testing method was adapted from ASTM E855 [16]. Strain measurements on the reinforcement and concrete surface, along with deflection measurements, were performed simultaneously using strain gauges and deflection gauges, respectively. This method was used to obtain detailed structural responses, similar to the approaches in the studies by Zhang et al. [3] and Hosen et al. [17]. Load, deflection, and strain data were continuously collected using a digital data acquisition system, which allowed for a dynamic analysis of the beam's behavior. Visual observations of failure modes, such as concrete spalling, cracking, and reinforcement fractures, were also recorded to complement the quantitative data, in accordance with the procedure recommended by [18]. This procedure ensures that the test results provide a thorough and valid evaluation of the beam performance.


Figure 3. Example of Tests on Reinforced Concrete Beams

### *2.4 Data Analysis and Performance Evaluation*

The analysis of the test data focused on evaluating the flexural capacity, ductility, and stiffness of the beams both before and after repair and strengthening. Load-deflection curves were compared between the control and repaired beams to quantify the improvement in flexural capacity, following the approach of [9], [18]. Ductility and stiffness were evaluated to assess changes in the deformation behavior of the beams resulting from the treatment, following the analysis methodology outlined by [19]. Additionally, the classification of failure modes, based on visual observations and test data, provided crucial insights into how the repair methods affected the failure mechanisms, as described by [20]. The results of this analysis form the basis for developing conclusions and technical recommendations that can be applied to the repair and strengthening of reinforced concrete structures in practice, thereby supporting the development of safer and more sustainable infrastructure.

P-ISSN: 1411-3414
E-ISSN: 2549-9815

## 3. Results and Discussion

### *3.1 Mechanical Characterization of GFRP Reinforced Materials Through Tensile Testing*

The GFRP reinforcement used was a Tyfo® The Fiberwrap Composite System SEH-51A product from Fyfe Company. Figure 4 shows the tensile testing conducted to characterize the mechanical properties of Glass Fiber Reinforced Polymer (GFRP) as a structural reinforcement material, in accordance with the ASTM D3039 standard. The GFRP specimens were fabricated using the hand layup method to simulate field conditions. They were then tested using a 1000 kN Universal Testing Machine (UTM) at a loading rate of 0.5 mm/sec to obtain a quasi-static response.

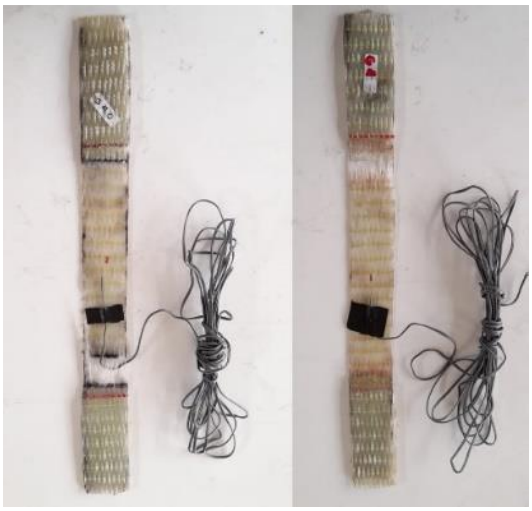

Figure 4. GFRP Tensile Strength Testing

The results showed an average tensile strength of 325.43 MPa, an ultimate strain of 6,512 με (which is 29.6% of the manufacturer's specification), and an elastic modulus of 5.00 GPa. These data indicate that the failure of the specimens was not caused by the breakage of GFRP fibers but rather by the degradation of the bond between the GFRP and concrete, a phenomenon known as debonding. This finding is consistent with the study by Jagadheeswari et al. [15], which evaluated the GFRP-concrete interface interaction in reinforced beams. This characterization provides a critical basis for understanding the load transfer mechanism and optimizing the reinforcement design to ensure long-term structural integrity By integrating experimental data with valid references, this approach provides a framework for anticipating material behavior under actual service conditions, similar to the method applied in Ghous Sohail et al. [19] study on reinforced concrete structures with GFRP.

### *3.2 Ultimate Load Capacity Analysis*

The evaluation of ultimate load capacity (Figure 5) revealed a significant difference in performance between the control beam (RB) and the repaired and reinforced beams. The control beam, denoted as BK, recorded an average maximum load of 29.74 kN. In contrast, the beam repaired solely with grouting (RBGR) showed a drastic reduction in capacity, reaching only 14.49 kN. This indicates that grouting alone was insufficient to restore the original strength. The addition of GFRP reinforcement provided substantial improvement. The RBGS (GFRP strip) configuration achieved a load capacity of 27.81 kN, which is close to the BK capacity. Meanwhile, the RBGT (GFRP U-wrap) configuration demonstrated the highest performance with 32.50 kN, surpassing the BK capacity by 9.27%. While this increase is below the 20-60% range reported in some studies, it confirms the effectiveness of GFRP, particularly the U-wrap configuration. This finding is supported by a study by Lokuge et al. [21], which showed an increase in load capacity of up to 45% in reinforced concrete beams reinforced with a GFRP U-wrap. Furthermore, the study by Jagadheeswari et al. [15] confirmed that reinforcement with GFRP significantly improved shear resistance and prevented early cracking in degraded concrete beams. The study by Ghous Sohail et al. [19] also highlighted the importance of the reinforcement configuration and the bond quality between the GFRP and concrete as significant factors in determining reinforcement effectiveness, which is consistent with the findings of this study. Table 1 presents the test results for all 12 specimens and details the changes observed in the beams after the repair variations.

P-ISSN: 1411-3414
E-ISSN: 2549-9815

Table 1. Ultimate Load Test Results

| Specimens | Code | Max Load. (kN) | Average Max Load (kN) | Percentage Increase (%) |
|---|---|---|---|---|
| Control Beam | RC 1 | 28.12 | 29.74 | - |
| | RC 2 | 30.45 | | |
| | RC 3 | 30.65 | | |
| Variety Beams | RBGR 1 | 14.73 | 14.39 | -51.6 |
| | RBGR 2 | 14,39 | | |
| | RBGR 3 | 14.06 | | |
| | RBGS 1 | 26.92 | 27.81 | -6.5 |
| | RBGS 2 | 28.92 | | |
| | RBGS 3 | 27.59 | | |
| | RBGT1 | 32.85 | 32.50 | 9.3 |
| | RBGT 2 | 30.25 | | |
| | RBGT 3 | 34.39 | | |

The low performance of RBGR beams is primarily attributed to the weak interface between the grout and the old concrete. Imperfect bonding can create weak zones, which trigger delamination under load and consequently hinder effective stress transfer. This phenomenon explains why RBGS and even RBGT beams, despite having their physical dimensions restored by grouting, fail to achieve the capacity of the control beam (RB). This phenomenon was also observed in a study by Abadel et al. [22], which found that debonding failure at the grout-concrete interface was the primary cause of structural capacity reduction in beams repaired without additional reinforcement.

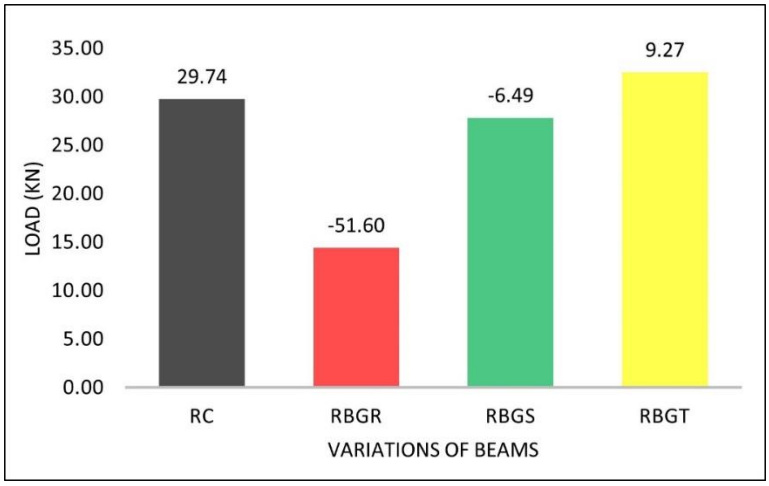


Figure 5. Comparison of Load Capacity Increase (%)

The success of GFRP reinforcement lies in its ability to withstand tensile stresses, even after the steel reinforcement has yielded, provided that the bond with the concrete is maintained. The superiority of the RBGT configuration suggests that additional reinforcement in the support area (U-wrap) is crucial. This is likely due to the increased shear resistance and confinement effect, which allows for better load distribution. Nevertheless, the effectiveness of GFRP is limited by the reinforcement design and bond quality. The debonding failures observed in this study (as discussed previously) prevented the GFRP from reaching its full strength potential, thereby confirming that bond integrity is a key determining factor.

### *3.3 FRP Strain Distribution*

The strain distribution in Fiber-Reinforced Polymer (FRP) materials used for concrete reinforcement is crucial for evaluating structural performance. The ACI 440.2R-17 standard serves as a key reference for understanding FRP strain distribution. According to Hooke's principle of elasticity, FRP strain is linear during the initial stages of loading. However, as loads increase, debonding can occur

at the FRP-concrete interface, leading to a non-linear strain distribution and a disproportionate increase in strain [23]. The identification of the debonding threshold is therefore crucial in the design of FRP reinforcement.

FRP strain distribution is influenced by several factors, including the FRP elastic modulus, cross-sectional dimensions, and tensile strength, as well as the adhesive characteristics, concrete dimensions, reinforcement configuration, and the mechanical properties of the concrete itself. The variability of these parameters makes accurate predictions challenging. Experimental data from GFRP-reinforced concrete beams (Figure 6) show a proportional strain distribution at low loads (10–25 kN). However, significant deviations occurred at higher loads (25–28.92 kN), which indicates the initiation of debonding in the mid-span area. Real-time strain monitoring is therefore essential for design validation and for ensuring long-term structural integrity.

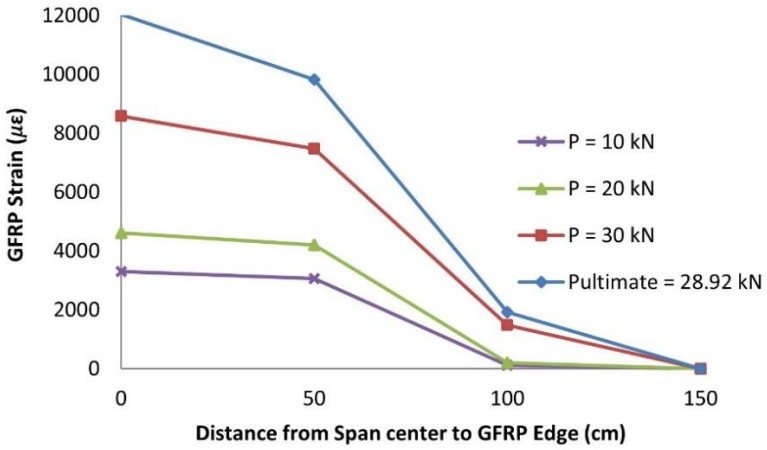


Figure 6. Strain Distribution of GFRP RBGS Beams

At the ultimate load of 28.92 kN, the GFRP strain reached 11616 με, which indicates that the GFRP began to debond from the concrete, propagating from the mid-span towards the support. Overall, the GFRP strain graph illustrates the good behavior of GFRP-concrete composite beams up to a load of 25 kN. Debonding began to occur at higher loads, leading to the detachment of the GFRP from the concrete. Research by Koushafar et al. [8] comprehensively discussed the debonding failure mechanism in FRP-reinforced concrete structures and found that debonding propagation often starts from the high-strain area at the center of the span, spreading toward the supports as the load increases. Similarly, research by Garcez et al. [24] observed that failure due to debonding was characterized by a rapid increase in FRP strain followed by the detachment of the FRP material from the concrete surface, particularly after exceeding a certain load threshold. This phenomenon further reinforces the importance of understanding debonding behavior in the design and analysis of concrete structures reinforced with FRP.

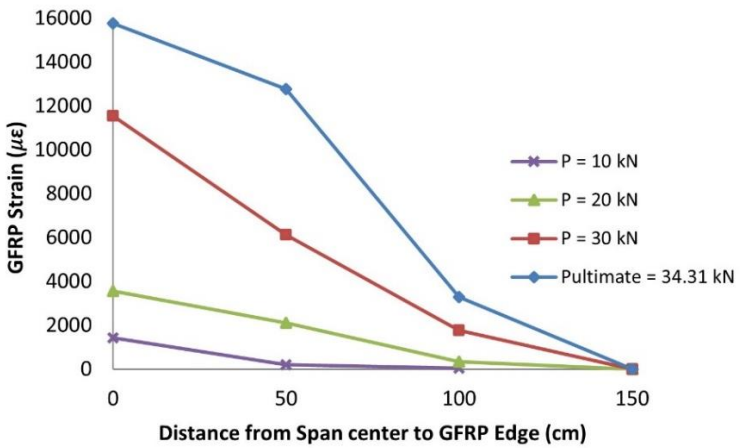


Figure 7. Strain Distribution of GFRP RBGT Beams

Figure 7 displays the strain distribution diagram for GFRP in RBGT beams, which were reinforced with GFRP on both sides of the support. This diagram shows a consistent pattern across various load levels. At early load levels, such as 10 kN (20-1500 με) and 20 kN (300-4000 με), the GFRP strain distribution exhibited linear behavior, which is consistent with the findings of Capozucca et al. [2] on FRP-reinforced concrete beams. However, once the load reached 30 kN (1700-12000 με), the strain distribution changed significantly, with a notable difference in strain values at the mid-span. This indicates the initiation of GFRP debonding, a phenomenon also observed by Capozucca et al. [25]. They noted that debonding typically begins in the area of highest interfacial strain and shear stress, which is often at the mid-span. Furthermore, Jagadheeswari et al. [15] and Mansur et al. [18] also reported changes in strain distribution as an early indication of debonding, emphasizing the importance of strain monitoring.

The RC beam of type RBGT reached an ultimate load of 34.31 kN, at which point the GFRP strain reached 15759 με. At this load, the GFRP debonded, propagating from the mid-span to the end of the pedestal. Although debonding occurred, the high ultimate load indicates that the addition of GFRP effectively increased both the strength and the ultimate capacity of the reinforced concrete. This analysis provides strong evidence that applying GFRP significantly improves the ability of reinforced concrete beams to withstand loads prior to cracking and propagation, thereby enhancing the overall structural flexural strength.

### *3.4 Crack Patterns in Reinforced Concrete Beams*

Flexural cracking was the dominant failure mode in all four beam types. It was characterized by vertical cracks that originated on the tensile side and propagated towards the neutral axis as the bending moment exceeded the beam's capacity. Crack initiation was generally observed in the middle third of the tensile span. These cracks then propagated intensively towards the compressive side as the load increased. At peak load, the cracks continued to expand, leading to significant widening and a loss of beam stiffness. The collapse was ductile, preceded by the yielding of the tensile reinforcement. The collapse was ductile, preceded by the yielding of the tensile reinforcement. Compared to the control beams, the GFRP-reinforced beams showed an increased load capacity before cracking and crack propagation [2]. This indicates that GFRP is effective in improving crack resistance and increasing the load capacity before ductile failure [9]. Although cracks widened and deflection increased at maximum load, the beams were still able to withstand the load before a significant decrease in capacity and a rapid increase in deflection occurred [24]. The observed flexural cracking patterns are consistent with the theoretical behavior of reinforced concrete beams under flexural loads.

Based on the observations in Figure 8, flexural crack initiation was detected at a load of 3.4 kN, signaling the beginning of significant elastic deformation in the beam material [13]. The yielding of the material was observed at a load of 26.18 kN, indicating that the elastic limit had been reached and plastic deformation had begun [4], [5]. Ultimate flexural failure occurred at a maximum load of 28.12 kN. It was characterized by beam fracture due to flexural stresses exceeding the beam's capacity and by a crack length that exceeded three-quarters of the span. After the maximum load, 25 crack patterns were identified. These cracks followed the direction of the bending stress, tended to be parallel to the load direction, and became localized and elongated as the load increased until final failure [10]. These crack patterns confirm that the dominant failure mechanism in RC beams was flexural.

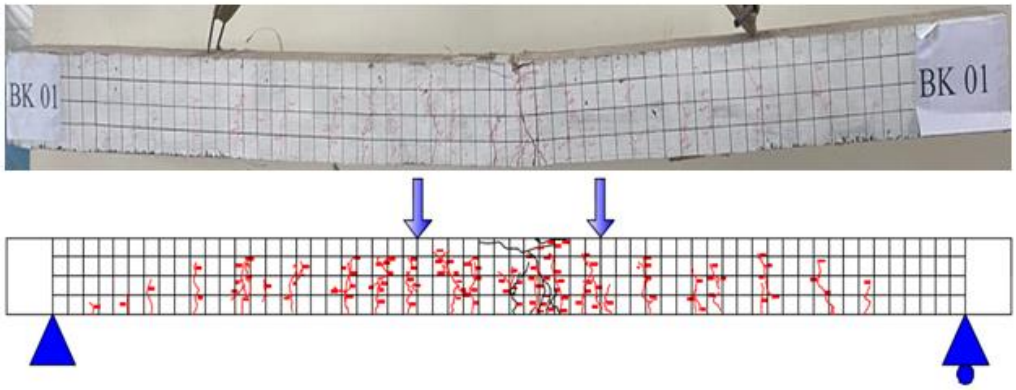


Figure 8. Crack Pattern of RC Concrete

P-ISSN: 1411-3414
E-ISSN: 2549-9815

Based on the observations in Figure 9, the first flexural crack in the RBGR specimens was detected at a load of 3.47 kN in the area of maximum bending moment. This indicates that the concrete's tensile strength had been exceeded [26]. As the load increased, this crack propagated vertically from the tensile side towards the neutral axis and widened. The yielding of the tensile reinforcement occurred at a load of 11.99 kN, which marked the beginning of inelastic behavior [27]. The maximum load of 14.73 kN was reached when the flexural cracking had extended beyond the neutral axis. In addition to vertical flexural cracking (with 18 branching grooves), horizontal cracks also formed along the old concrete and grouting joints. This indicates premature delamination caused by poor interface adhesion [19], [28]. After exceeding the maximum load, the beam experienced a ductile collapse, characterized by excessive deformation (deflection) and cross-sectional damage.

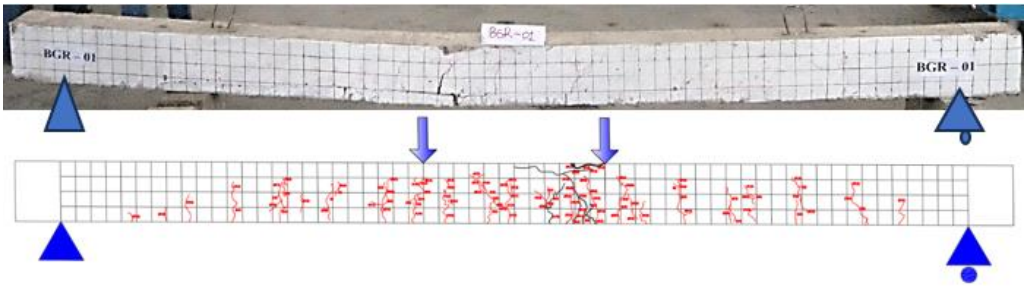


Figure 9. Crack Pattern of Concrete Block RBGR

Figure 10 shows an RBGS beam with post-grouting spalling that was initially without cracks. The first flexural crack was observed at a load of 7.86 kN in the maximum moment area. This crack developed vertically towards the mid-span, resulting in 21 crack patterns. The higher number of cracks compared to the RBGR beams indicates increased stiffness due to the GFRP reinforcement, which resulted in tighter cracking (ACI 440.2R-17). The maximum load for the RBGS beam reached 26.92 kN, which is approximately 15% higher than that of the RBGR beam. This finding proves the effectiveness of GFRP as an external flexural reinforcement in increasing load capacity [26], [29]. During vertical crack propagation, several small cracks merged into a dominant crack. Horizontal cracking and grouting were also observed at the interface of the old concrete, indicating potential adhesion problems. Material yielding occurred at a load of 19.79 kN, before the beam reached its maximum load of 26.92 kN. At the maximum load, a sudden release of the GFRP, accompanied by a loud noise, occurred as the GFRP attempted to resist the load after the steel reinforcement had yielded. Vertical cracks extended beyond the neutral axis and horizontal cracks widened, leading to structural failure of the RBGS beams. This failure was characterized by complete collapse and detachment of the GFRP.

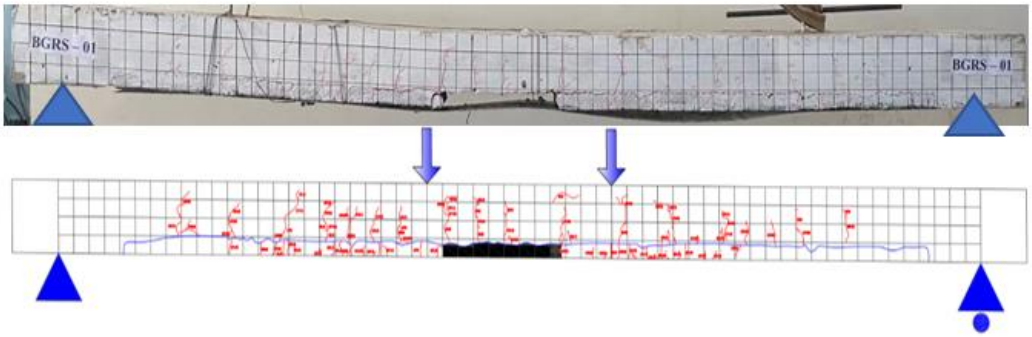


Figure 10. Crack Pattern of RBGS Concrete Beams

Figure 11 shows that the first flexural crack in the RBGT beam occurred at a load of 9.86 kN in the area of maximum bending moment (approximately one-third of the span). This was caused by the tensile stress exceeding the tensile strength of the concrete [14]. The increased load caused the vertical propagation and widening of flexural cracks from the tensile side to the compressive side. Transverse cracking at the contact area indicated delamination between the old concrete and the grouting. The yielding of the tensile reinforcement occurred at a load of 19.53 kN, which could have led to the debonding of the reinforcement [30]. As the maximum load was approached, the tensile stress in the

GFRP layer exceeded the adhesive strength. This triggered vertical flexural cracking (visible as white grooves) on the GFRP surface in the mid-span area, signaling a potential GFRP tear at the ultimate load.

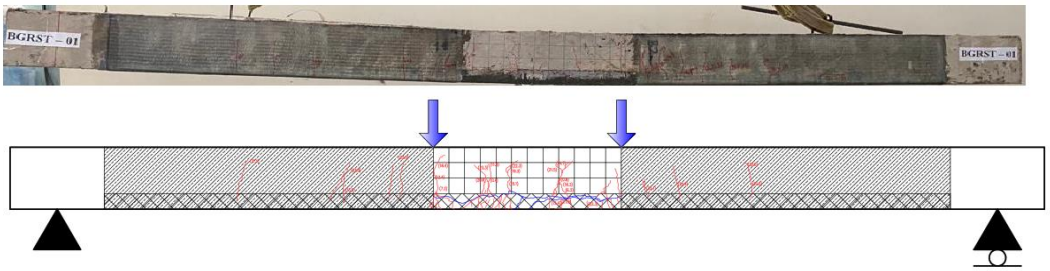


Figure 11. Crack Pattern of RBGT Concrete Beams

The cracking pattern in the GFRP-covered concrete, with 17 flexural cracks observed in both the concrete and GFRP, indicated that crack propagation extended almost throughout the entire cross-section. The addition of GFRP to the RBGT beams significantly reduced the flexural cracking (by 30-40%) compared to the RBGS and RBGR beams, which is attributed to the increased flexural stiffness. The maximum load of 34.39 kN was reached when the flexural cracking extended beyond the neutral axis (approximately three-quarters of the span). This was followed by a ductile collapse after the complete detachment of the GFRP layers.

## 4. Conclusion

This study comprehensively demonstrates the effectiveness of a combined repair strategy, which involves grouting and Glass Fiber Reinforced Polymer (GFRP) reinforcement, in improving the structural performance of deteriorated reinforced concrete beams. The main findings show that the application of GFRP reinforcement, particularly in a U-wrap configuration, provides a significant increase in the beams' flexural capacity. The 9.27% increase in the average maximum load (from 29.74 kN in control beams to 32.50 kN in RBGT beams) confirms the potential of GFRP as an effective retrofitting solution. In contrast, a standalone grouting application could not restore the initial strength. It even tended to decrease the load capacity substantially (to a mere 14.49 kN), indicating the limitations of grouting as a single structural repair method for significant damage. Further analysis revealed that debonding failure at the grout-concrete interface is a critical factor hindering the effectiveness of a standalone grouting repair. A comparison of GFRP reinforcement configurations highlighted the superiority of the U-wrap (RBGT) over the strip (RBGS) configuration. This is likely due to the U-wrap's contribution to improved shear resistance and better confinement of the critical flexural zone. Observations of crack patterns showed that adding GFRP effectively reduced the propagation and number of flexural cracks. This coincided with an increase in collapse ductility, which was generally preceded by the yielding of the tensile reinforcement. In conclusion, this study advocates for a combined strategy of grouting to fill cracks and using GFRP reinforcement, especially in a U-wrap configuration, as a promising approach for rehabilitating damaged reinforced concrete beams. However, this study also emphasizes the importance of achieving a strong and durable bond between the repair material and the concrete substrate to mitigate the risk of debonding and ensure the realization of the full potential of this repair technique. The implications of these findings are significant for structural engineering practice, particularly for repairing and maintaining aging concrete infrastructure. Future research is recommended to explore methods for improving interfacial adhesion and for optimizing GFRP configurations for different levels of deterioration and various environmental conditions.

## Acknowledgments

This research was funded through the 2025 DIPA Research Program for Lecturers from the Institute for Research and Community Service (LP2M) at the University of Borneo Tarakan. The author is profoundly grateful for the support.

## References

[1] T. Siwowski, M. Rajchel, and L. Wlasak, “Experimental study on static and dynamic performance

of a novel GFRP bridge girder," *Compos Struct*, vol. 259, p. 113464, Mar. 2021, doi: 10.1016/J.COMPSTRUCT.2020.113464.

[2] R. Capozucca, E. Magagnini, and E. Bettucci, "Delamination buckling of GFRP-strips in strengthened RC beams," *Compos Struct*, vol. 300, p. 116183, Nov. 2022, doi: 10.1016/J.COMPSTRUCT.2022.116183.

[3] X. Zhang, L. Wang, J. Zhang, and Y. Liu, "Corrosion-induced flexural behavior degradation of locally ungrouted post-tensioned concrete beams," *Constr Build Mater*, vol. 134, pp. 7–17, Mar. 2017, doi: 10.1016/j.conbuildmat.2016.12.140.

[4] H. Alsuwaidi *et al.*, "Evaluation and Restoration of Corrosion-Damaged Post-Tensioned Concrete Structures," *Civil Engineering Journal (Iran)*, vol. 10, no. 12, pp. 3834–3850, Dec. 2024, doi: 10.28991/CEJ-2024-010-12-02.

[5] H. Luan, Y. Fan, L. Zhao, X. Ju, and S. P. Shah, "Corrosion characteristics and critical corrosion depth model of reinforcement at concrete cover cracking in an electrochemical accelerated corrosion environment," *Case Studies in Construction Materials*, vol. 22, Jul. 2025, doi: 10.1016/jcscm2025e04628.

[6] T. G. Wakjira and U. Ebead, "Strengthening of reinforced concrete beams in shear using different steel reinforced grout techniques," *Structural Concrete*, vol. 22, no. 2, pp. 1113–1127, Apr. 2021, doi: 10.1002/SUCO.202000354.

[7] R. Capozucca, E. Magagnini, and E. Bettucci, "Delamination buckling of GFRP-strips in strengthened RC beams," *Compos Struct*, vol. 300, Nov. 2022, doi: 10.1016/j.compstruct.2022.116183.

[8] K. Koushfar *et al.*, "Behavior of grouted splice sleeve connection using FRP sheet," *Eng Struct*, vol. 296, p. 116898, Dec. 2023, doi: 10.1016/J.ENGSTRUCT.2023.116898.

[9] F. Gong, X. Jiang, Y. Gamil, B. Iftikhar, and B. S. Thomas, "An overview on spalling behavior, mechanism, residual strength and microstructure of fiber reinforced concrete under high temperatures," *Front. Mater.*, vol. 10, p. 1258195, Sep. 2023, doi: 10.3389/FMATS.2023.1258195/XML.

[10] M. M. Attia, B. A. Abdelsalam, D. E. Tobbala, and B. O. Rageh, "Flexural behavior of strengthened concrete beams with multiple retrofitting systems," *Case Studies in Construction Materials*, vol. 18, Jul. 2023, doi: 101016/j.cscm.2023e01862.

[11] R. Afanda and A. Zaki, "Effects of Repair Grouting and Jacketing on Corrosion Concrete Using Ultrasonic Method," *SDHM Structural Durability and Health Monitoring*, vol. 19, no. 2, pp. 265–284, Jan. 2025, doi: 10.32604/SDHM.2024.053084.

[12] Z. H. Lu, Q. H. Zhou, H. Li, and Y. G. Zhao, "A new empirical model for residual flexural capacity of corroded post-tensioned prestressed concrete beams," *Structures*, vol. 34, pp. 4308–4321, Dec. 2021, doi: 10.1016/j.istruc.2021.10.005.

[13] J. Taheri-Shakib and A. Al-Mayah, "Dynamics of localized accelerated corrosion in reinforced concrete: Voids, corrosion products, and crack formation," *Ceram Int*, vol. 50, no. 22, pp. 48755–48767, Nov. 2024, doi: 10.1016/J.CERAMINT.2024.09.229.

[14] K. Koushfar *et al.*, "Behavior of grouted splice sleeve connection using FRP sheet," *Eng Struct*, vol. 296, p. 116898, Dec. 2023, doi: 10.1016/J.ENGSTRUCT.2023.116898.

[15] Jagadheeswari, Sivarethinamohan, Muthumari, Ramalakshmi, Ilayaraja, and Z. Rahman, "Strength and ductility behaviour of FRC beams strengthened with externally bonded GFRP laminates," *Mater Today Proc*, vol. 37, no. Part 2, pp. 2542–2546, Jan. 2021, doi: 10.1016/J.MATPR.2020.08.491.

[16] M. H. El-Naqeeb, R. Hassanli, Y. Zhuge, X. Ma, M. Bazli, and A. Manalo, "Beam-column connections in GFRP-RC moment resisting frames: A review of seismic behaviour and key parameters," *Structures*, vol. 71, p. 108109, Jan. 2025, doi: 10.1016/J.ISTRUC.2024.108109.

[17] M. A. Hosen *et al.*, "Effect of bonding materials on the flexural improvement in RC beams strengthened with SNSM technique using GFRP bars," *Journal of Building Engineering*, vol. 32, Nov. 2020, doi: 10.1016/j.jobe.2020.101777.

[18] A. Z. Mansur, R. Djamaluddin, H. Parung, R. Irmawaty, and D. Nawir, "Civil Engineering Journal Effectiveness of Grouting and GFRP Reinforcement for Repairing Spalled Reinforced Concrete Beams," 2024, doi: 10.28991/CEJ-2024-010-07-05.

[19] M. Ghous Sohail, M. Wasee, N. Al Nuaimi, W. Alnahhal, and M. K. Hassan, "Behavior of artificially corroded RC beams strengthened with CFRP and hybrid CFRP-GFRP laminates," *Eng Struct*, vol. 272, p. 114827, Dec. 2022, doi: 10.1016/J.ENGSTRUCT.2022.114827.

[20] M. A. El-mandouh, M. S. Omar, M. A. Elnaggar, and A. S. Abd El-Maula, "Cyclic Behavior of High-Strength Lightweight Concrete Exterior Beam-Column Connections Reinforced with GFRP," *Buildings*, vol. 12, no. 2, Feb. 2022, doi: 10.3390/BUILDINGS12020179.

[21] W. Lokuge, O. Otoom, R. Borzou, S. Navaratnam, N. Herath, and D. Thambiratnam, "Experimental and numerical analysis on the effectiveness of GFRP wrapping system on timber pile rehabilitation," *Case Studies in Construction Materials*, vol. 15, p. e00552, Dec. 2021, doi: 101016/J.CSCM.2021E00552.

[22] A. Abadel, H. Abbas, A. Albidah, T. Almusallam, and Y. Al-Salloum, "Effectiveness of GFRP strengthening of normal and high strength fiber reinforced concrete after exposure to heating and cooling," *Engineering Science and Technology, an International Journal*, vol. 36, p. 101147, Dec. 2022, doi: 10.1016/J.JESTCH.2022.101147.

[23] T. Siwowski, H. Zobel, T. Al-Khafaji, and W. Karwowski, "FRP bridges in Poland: State of practice," *Archives of Civil Engineering*, vol. 67, no. 3, pp. 5–27, 2021, doi: 10.24425/ACE.2021.138040.

[24] M. R. Garcez, L. C. Meneghetti, and R. M. Teixeira, "The effect of FRP prestressing on the fatigue performance of strengthened RC beams," *Structural Concrete*, vol. 22, no. 1, pp. 6–21, Feb. 2021, doi: 10.1002/SUCO.201900079.

[25] R. Capozucca and E. Magagnini, "Experimental response of masonry walls in-plane loading strengthened with GFRP strips," *Compos Struct*, vol. 235, Mar. 2020, doi: 10.1016/j.compstruct.2019.111735.

[26] T. Pan *et al.*, "Damage pattern recognition for corroded beams strengthened by CFRP anchorage system based on acoustic emission techniques," *Constr Build Mater*, vol. 406, Nov. 2023, doi: 10.1016/j.conbuildmat.2023.133474.

[27] Y. Kusuma, T. Rashmi, V. N. Anand, and N. C. Balaji, "An experimental study on flexural performance of RC beams strengthened by NSM technique using GFRP strips for a resilient infrastructure system," *Mater Today Proc*, vol. 52, pp. 1959–1967, Jan. 2022, doi: 10.1016/J.MATPR.2021.11.600.

[28] Z. Xiong, C. Zhao, Y. Meng, and W. Li, "A damage model based on Tsai–Wu criterion and size effect investigation of pultruded GFRP," *Mechanics of Advanced Materials and Structures*, vol. 31, no. 3, pp. 571–585, 2024, doi: 10.1080/15376494.2022.2116754.

[29] R. Xia, C. Jia, and Y. Garbatov, "Deterioration of marine offshore structures and subsea installations subjected to severely corrosive environment: A review," *Materials and Corrosion*, 2024, doi: 10.1002/maco202314050;csubtype:string:ahead

[30] N. M. Ayash, A. M. Abd-Elrahman, and A. E. Soliman, "Repairing and strengthening of reinforced concrete cantilever slabs using Glass Fiber–Reinforced Polymer (GFRP) wraps," *Structures*, vol. 28, pp. 2488–2506, Dec. 2020, doi: 10.1016/j.istruc.2020.10.053.